

Vacancy-related centers in diamond

Gordon Davies, Simon C. Lawson,* Alan T. Collins, Alison Mainwood, and Sarah J. Sharp
Physics Department, King's College London, The Strand, London WC2R 2LS, United Kingdom

(Received 4 June 1992)

It is established that vacancies in diamond migrate, during annealing, primarily in their neutral charge state, with an activation energy of 2.3 ± 0.3 eV. Negative vacancies are destroyed by first converting to neutral centers in a reversible charge transfer process. In relatively pure diamonds (type IIa) and in diamonds (type I) containing large concentrations of nitrogen, effectively all the vacancies in the samples after irradiation can be accounted for in their neutral (V^0) and negative (V^-) charge states. In nitrogen-rich diamonds, the vacancies are predominantly trapped during annealing at the nitrogen. From the annealing data we derive the relative oscillator strengths of the main absorption bands of V^0 , V^- , and of one vacancy combined either with a single N atom, a pair of N atoms, or the larger "B" aggregate of nitrogen. In the absence of the intrinsic nonradiative decay channels of luminescence from V^0 , we show that the radiative decay time would be 35 ± 7 ns. In common natural ("type IaA") diamonds, variations of absorption linewidths during annealing imply that about 40% of the vacancies are created within a few atomic sites of the nitrogen impurity, and direct observation confirms that vacancy production is enhanced in these diamonds. About half the vacancies, including those created near the nitrogen, anneal at each temperature about 12 times faster than those vacancies whose creation is not correlated with the nitrogen.

I. INTRODUCTION

The first systematic studies of radiation damage in diamond¹ were published in the 1950s. Since then extensive optical and paramagnetic resonance studies have produced a considerable amount of information on the radiation damage centers, as reviewed in Ref. 2. In this paper we are concerned primarily with vacancies. The neutral vacancy is nonparamagnetic but has been thoroughly investigated through its optical absorption/luminescence system.³ This system, known as the "GR1 band," has its zero-phonon line at 1.673 eV, Fig. 1(a). Uniaxial stress perturbations of the zero-phonon line have shown that the GR1 transition occurs at a center with the full tetrahedral symmetry of the substitutional site.⁴ The transition is between a ground orbital state which is doubly degenerate (irreducible representation E) and a triply degenerate orbital excited state (of T_2 or T_1 representation). Both the ground and excited states undergo Jahn-Teller relaxations, but the effects are dynamic and V^0 maintains the T_d point group of an atomic site in diamond.⁵ Additional transitions from the same E ground state produce a set of at least 12 sharp absorption lines at photon energies of 2.88–3.04 eV, merging into an absorption continuum.⁶ These excited states are suggestive of excitation into a series of shallow bound states of V^0 . Photo-Hall measurements on the carrier ionized from these states show that it is a hole, locating the excited states near the valence band.⁷ Consequently the ground state of V^0 is located close to the center of the energy gap of perfect diamond, which is $E_g \sim 5.49$ eV.⁸ The radiative decay time of the GR1 photoluminescence band is 2.55 ± 0.1 ns in the limit of low temperature. It decreases with increasing temperature, showing that there are strongly competing nonradiative deexcitation channels.⁹

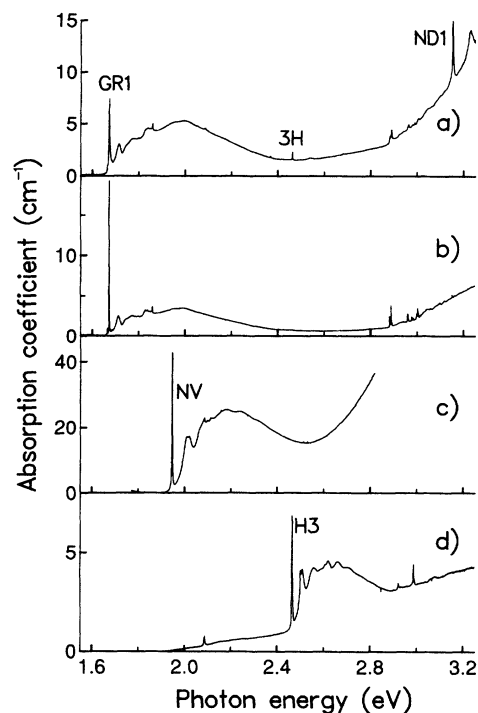


FIG. 1. Representative spectra, recorded at liquid-nitrogen temperature, of (a) a type IaA diamond after irradiation at nominal room temperature with 3×10^{17} 2-MeV electrons cm^{-2} ; (b) a type IIa diamond irradiated under the same conditions as the sample in (a); (c) a type Ib sample after irradiation and annealing; (d) a type IaA diamond after irradiation and annealing. To generate a measurable NV vibronic band, the sample used in (c) was chosen to have a higher nitrogen content and a higher dose than the Ib samples used in the annealing studies.

The singly negative charged state of the vacancy, V^- , has recently been identified by paramagnetic resonance measurements,¹⁰ but most studies of V^- have been carried out using its characteristic optical absorption band, the "ND1 band" with its zero-phonon line at 3.150 eV (Ref. 11) [Fig. 1(a)]. Like the GR1 band, the ND1 absorption band also occurs at a T_d center, from an orbital nondegenerate 4A state to a triply degenerate orbital state.¹² There is no ND1 photoluminescence band; instead the center deexcites by emission of a charge (of unknown sign) producing an ND1 photoconduction spectrum.¹³ It has been reported¹⁴ that intense illumination in the ND1 band reduces its strength, and increases the GR1 band; heating in the dark reverses these changes.

The equilibrium charge state of a vacancy in any diamond is controlled by the major impurities in that diamond. In relatively pure diamonds, referred to as "type IIa" diamonds, the GR1 absorption is far stronger than the negligible ND1 absorption [Fig. 1(b)], implying that the equilibrium charge state is neutral rather than negative.¹¹ Most natural diamonds contain nitrogen at a concentration of about 10^{19} cm^{-3} (Ref. 15), with other impurities at concentrations several orders of magnitude smaller. The nitrogen may be present in several different atomic structures, which are identifiable by their characteristic absorption bands.^{16,17} The smallest structure is when one nitrogen atom substitutes for one carbon atom, producing what is referred to as "type Ib" diamond. The N atom is known to undergo a relaxation to take up C_{3v} symmetry by lengthening one of the N-C bonds.¹⁸⁻²⁰ It is a donor with an ionization energy of $E_d \sim 1.9 \text{ eV}$,²¹ resulting in V^- being the favored charge state in type Ib diamonds¹¹ to the extent that in some natural type Ib diamonds the ratio of GR1 absorption (characteristic of V^0) to the ND1 absorption (characteristic of V^-) may approach zero.²² In type Ib diamonds synthesized at high pressure, the charge equilibrium is expected to be affected by the very different nitrogen concentrations in different growth sectors.²³

Only a very small proportion of natural diamonds is of type Ib because, despite the migration energy of nitrogen being $5.0 \pm 0.3 \text{ eV}$, significant motion of the N atoms occurs over geological time spans, allowing the N atoms to aggregate.²⁴ The smallest aggregate, the "A aggregate," is commonly found in natural diamonds and consists of two nearest neighbor substitutional nitrogen atoms.²⁵ It is a very deep donor with an ionization energy of $\sim 4 \text{ eV}$.²⁶ Further aggregation of the nitrogen produces a larger complex, the "B aggregate," and usually planar defects ("platelets") are created simultaneously. There are no data on the ionization energy of the B aggregate. The two vacancy charge states V^0 and V^- coexist in type Ia diamonds containing any combination of the A and B nitrogen aggregates, and their respective absorption bands have similar strengths [Fig. 1(a)].

Vacancies in diamond are static at room temperatures. In contrast, the self-interstitial, which is believed to be a $\langle 001 \rangle$ split interstitial,²⁷ probably migrates during electron irradiation at about 50 K, producing interstitial-related paramagnetic centers^{28,29} and at larger doses forming interstitial loops.³⁰ No optical signal has yet

been definitely associated with self-interstitials. One signature of a self-interstitial may be local vibrational modes involving a carbon atom, as is observed at several optical centers produced by radiation damage plus some annealing.³¹ However, the situation is confused since it is known that vacancy-related centers in diamond may show local modes involving carbon.³² In the present paper the self-interstitials are not important—we will see no evidence for reactions between vacancies and self-interstitials, except possibly in the earliest stages of annealing type IIa diamonds (Sec. IV).

When the relatively pure type IIa diamond is annealed at 600°C , the GR1 band of V^0 is destroyed. Its destruction has been correlated with the growth of the "TH5" optical band, and it has been suggested that TH5 occurs at a divacancy.¹ At higher annealing temperatures TH5 is unstable, but at least some of the vacancies aggregate in chains approximately along $\langle 110 \rangle$ axes, creating paramagnetic centers.³³ Type IIa diamonds contain dislocations at typical densities of 10^8 cm^{-2} (Ref. 34) and their importance in trapping vacancies is not known.

In type Ib diamonds, annealing destroys the ND1 and any GR1 absorption as the vacancies migrate to, and are trapped at, the single substitutional nitrogen atoms.²² The resulting nitrogen-vacancy pair (N-V) has the expected C_{3v} symmetry. An optical transition between the ground orbital single state and the excited orbital doublet state produces the characteristic zero-phonon line at 1.945 eV [Fig. 1(c)]. Its radiative decay time of $13 \pm 0.5 \text{ ns}$ is temperature independent between 77 and 700 K.³⁵ Recently this transition has been studied in hole-burning experiments.³⁶ The center also produces a paramagnetic resonance signal, whose properties confirm the C_{3v} symmetry.³⁷

It is well established that in type Ia diamonds the vacancies migrate to and are trapped at A or B nitrogen aggregates.³⁸ A vacancy trapped at an A aggregate produces absorption in the "H3" band with its zero-phonon line at 2.463 eV; trapped at a B aggregate it gives absorption at 2.498 eV in the "H4" band. Both the H3 and H4 centers are highly stable at the temperatures used in this work.³⁹ In a typical type Ia diamond with both A and B aggregates the H3 and H4 centers are produced in proportion to the A and B aggregates.³⁸ The H3 absorption band is shown in Fig. 1(d), and the band shape of H4 is very similar but is displaced $\sim 35 \text{ meV}$ to higher energy. H3 and H4 have very similar responses to uniaxial stresses.^{40,41} The point group of the H3 center is C_{2v} and that of H4 is C_{1h} (Refs. 40 and 41). These data indicate that H4 is a lower symmetry version of H3, the lowered symmetry resulting from the extra nitrogen atoms in the B nitrogen aggregate required to produce H4. The radiative decay times of the H3 and H4 photoluminescence bands are also very similar,^{42,43} at $16.7 \pm 0.5 \text{ ns}$ for H3 and $19.1 \pm 1 \text{ ns}$ for H4, and it is known that neither is temperature dependent.

Although our knowledge about the individual vacancy-related centers is considerable we do not have a quantitative understanding of the vacancy reactions during annealing. In this work we have exploited the effects of the different nitrogen impurity structures available in

diamond. In type IIa diamond, which approximates to pure diamond, V^0 predominates over V^- ; in type Ib diamond V^- is found in preference to V^0 ; and in type Ia diamond V^0 and V^- coexist. We will derive the migration energy of V^0 , and show that in the common type Ia diamond the migration of the vacancy is mediated through V^0 , with V^- centers decaying by first undergoing charge conversion to V^0 . By combining the data with the measured radiative decay times of the vacancy-related bands, we will suggest that in nitrogen-rich diamonds the nitrogen is the dominant trap for the migrating vacancies and that all the vacancies can be accounted for in terms of their neutral and negative charge states. We will show that in type Ia diamond the concentration of V^0 always exceeds that of V^- , partially explaining the failure to detect V^- in recent positron annihilation measurements.⁴⁴

II. SAMPLES AND EXPERIMENTAL DETAILS

Samples of types Ia, IIa, and Ib diamond have been used in this work. The type IIa (relatively pure) natural diamonds were chosen to contain negligible nitrogen (in practice less than $\sim 10^{17} \text{ cm}^{-3}$) on the basis of the lack of one-phonon optical absorption. We have chosen type Ia natural diamonds (containing nitrogen in the *A* and *B* aggregated forms) so that either the *A* aggregates or the *B* aggregates dominated in capturing the mobile vacancies. We will follow the convention of referring to these diamonds as type IaA and type IaB diamonds, respectively. They had between $(3.5 \text{ and } 6.2) \times 10^{19} \text{ cm}^{-3}$ nitrogen in the *A* form, and between $(0.03 \text{ and } 1.8) \times 10^{19} \text{ cm}^{-3}$ nitrogen in the *B* form, as measured from the optical absorption in the one lattice-phonon region.¹⁶ In the type IaA sample with the highest ratio of the concentrations of *B* to *A* nitrogen, $N_B/N_A = 0.29$, the ratio of absorption generated in the H4 and H3 zero-phonon lines was $A_{H4}/A_{H3} = 7 \times 10^{-2}$. This is consistent with earlier correlations³⁸ of the absorption coefficients integrated across the H4 and H3 zero-phonon lines [in the manner detailed below in Eq. (2.3)]:

$$A_{H4}/A_{H3} = 0.25 N_B/N_A . \quad (2.1)$$

Since the H3 and H4 bands are almost identical, the *A* aggregates dominated over the *B* aggregates for capturing vacancies in all our type IaA samples.

Three type IaB natural diamonds have been used with nitrogen concentrations in the *B* aggregated form of between $(1.6 \text{ and } 2.0) \times 10^{20} \text{ cm}^{-3}$, and in the *A* form of less than $3 \times 10^{18} \text{ cm}^{-3}$. A further three type IaB diamonds of lower nitrogen concentrations ($1.3 \text{ to } 8) \times 10^{19} \text{ cm}^{-3}$ but also of significantly worse crystal morphology have been examined.

The type Ib diamonds were synthetic diamonds grown with a getter to reduce the concentration of nitrogen substantially below the level found in commercial synthetic diamonds so that they were optically transparent in the region of the ND1 zero-phonon line. From the optical absorption in the ultraviolet,¹⁷ the mean nitrogen concentration was estimated to be $2 \times 10^{18} \text{ cm}^{-3}$, but with considerable variations in the different growth sectors.

All the diamonds were about 1.5 mm thick. They were irradiated at nominal room temperature with doses of $10^{16} - 10^{17} \text{ cm}^{-2}$ 2-MeV electrons. Irradiations carried out at nominal room temperature in rare natural semi-conducting diamond show that the rate of loss of the active boron acceptors is⁴⁵

$$\Delta p = -0.27 \text{ cm}^{-1} , \quad (2.2)$$

implying that the rate of production of damage centers is of this order. A similar figure (0.3 cm^{-1}) for vacancy production by 3.5-MeV irradiations has been derived recently using positron annihilation data.⁴⁴ In the work reported here the radiation doses are small enough that the concentration of V^0 centers is linearly proportional to the radiation dose.⁴⁶

The samples were annealed at temperatures between 600 and 800°C in a quartz tube evacuated to 10^{-5} Torr to prevent graphitization. The upper limit on the temperature was fixed by the need to keep the heating time of the tube substantially less than the anneal times, and the lower limit by the need for an acceptably quick result.

Absorption spectra were recorded with the samples at 77 K in the full white light of a tungsten lamp. Order sorting for the dispersive monochromator was by filters placed after the sample. From the representative spectra of Fig. 1 it is clear that the total absorption in the vibronic bands is difficult to measure since the absorption continuum underlying each band cannot be defined unambiguously. In contrast, the zero-phonon lines can be easily defined. Consequently in all cases we have measured the strength of absorption *A* for each band by integrating the absorption coefficient $\mu(E)$ (measured in cm^{-1}) at photon energy *E* (measured in meV) over the relevant zero-phonon line:

$$A = \int_{ZPL} dE \mu(E) . \quad (2.3)$$

III. OVERVIEW OF THE DATA

In this section we present results based on the isothermal annealing of four type IIa diamonds, eight type IaA diamonds, and three type Ib diamonds, and on the isochronal annealing of three type IaB diamonds. The data are introduced with the minimum of analysis, and they will be analyzed in detail in Secs. IV–IX.

A. Type IIa diamond

Electron irradiation of type IIa diamonds creates the GR1 band of V^0 , but negligible ND1 absorption of V^- [Fig. 1(b)]. On annealing between temperatures of 600 and 750°C about 30–50% of the GR1 line decays during the first stage of annealing. This process is too rapid for us to measure at these temperatures (Fig. 2), but in this paper we will be primarily concerned with the remaining GR1 absorption which decays with half-lives between 1.5 and 200 h. In all our type IIa diamonds the full widths at half height of the GR1 line were 4.4–5.1 meV and remained constant throughout the annealing.

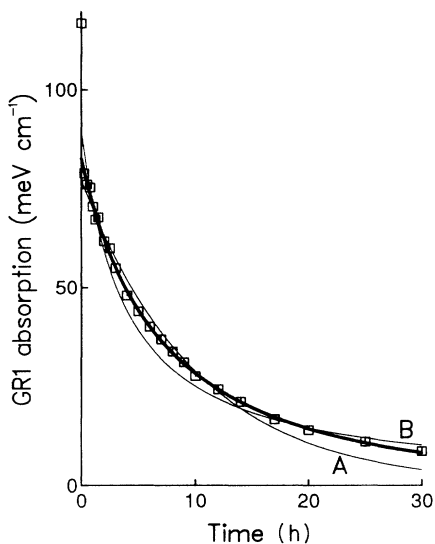


FIG. 2. Experimental points show the decrease in GR1 intensity during the annealing at 700°C of a type IaA diamond. The lines show calculated fits to the slower decay process, i.e., ignoring the point measured before annealing. Fits of first- and second-order kinetics are shown by lines labeled *A* and *B*, respectively. The thick line is calculated using Eq. (4.3) with the $1/r_1 = 25$ h and $r_2 = 1.43 \times 10^{-3} \text{ h}^{-1} \text{ meV}^{-1} \text{ cm}$.

B. Type IaA diamond

After electron irradiation the absorption spectra are dominated by the GR1 and the ND1 bands [Fig. 1(a)] with strengths closely proportional to each other [Fig. 3(a)]:

$$A_{\text{ND1}} / A_{\text{GR1}} = 0.53 \pm 0.03 \quad (3.1)$$

The ratio of GR1 and ND1 absorptions may change during annealing [Fig. 4(a)]. In the type IaA samples with low damage (corresponding to $A_{\text{GR1}} < 60 \text{ meV cm}^{-1}$), the ND1 and GR1 absorptions are almost proportional to each other during the annealing. However, samples with larger doses show an increase in ND1 absorption in the first stages of annealing, while the GR1 line decreases monotonically. This effect has been reported without comment earlier.⁴⁷ In Sec. VI we will associate it with charge transfer effects between V^0 and V^- .

On annealing each type Ia sample the H3 absorption was generated simultaneously with the loss of GR1 absorption (Figs. 5 and 6). There was a direct correlation between the loss of GR1 and the growth of H3 absorptions in all the samples, but not between the loss of ND1 and the growth of H3 [Fig. 3(b)].

One striking feature during the annealing of all the type IaA samples was that the full widths measured at half height of the GR1 and ND1 lines decreased during the first stages of annealing [Figs. 6(b) and 6(c)]. The H3 linewidth was either constant during the annealing, as in Fig. 6(b), or showed very small increases or decreases; however, the changes were always much smaller than for the GR1 and ND1 lines.

C. Type IaB diamond

Three type IaB diamonds, containing over $1.6 \times 10^{20} \text{ cm}^{-3}$ nitrogen in the B aggregates, have been annealed isochronally (1 h at each stage). In each diamond the H4 absorption produced during annealing was at least 14 times larger than the production of H3 absorption. Since the H3 and H4 bands are almost identical (Sec. I) we have allowed for the small H3 production by plotting the growth of H4 plus H3 absorption in Fig. 7. As for the type IaA diamonds the loss of GR1 absorption mirrors the growth of the end product (the H4 band here) in these diamonds with high nitrogen content. Three type IaB diamonds with lower nitrogen content ($8 \times 10^{19} \text{ cm}^{-3}$) have also been annealed. For these samples the production of H4 absorption was up to 2.2 times smaller, relative to the initial damage, than for the type IaB diamonds with higher nitrogen. We will not discuss these samples further, except to note that in natural diamonds which contain slip planes and platelets as well as nitrogen, the vacancies are not predominantly trapped at the nitrogen.

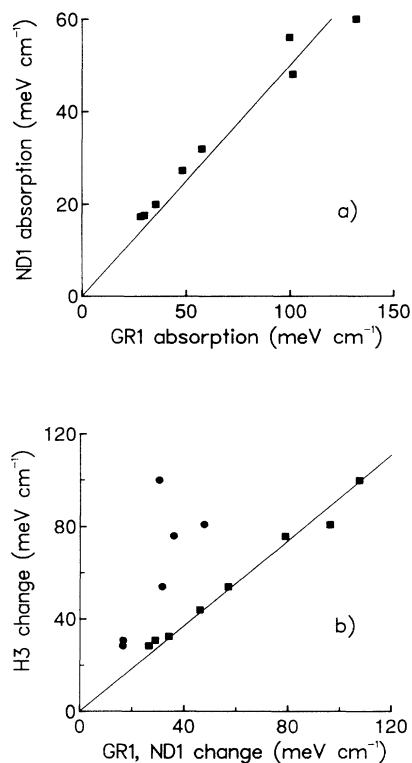


FIG. 3. (a) Experimental data for the strengths of absorption in the ND1 and GR1 lines (of V^- and V^0 , respectively), after irradiation and before annealing, measured in eight type IaA diamonds. (b) Data from eight type IaA diamonds for the changes in absorption during isothermal annealing. Squares compare experimental data for the reduction in absorption in the GR1 line with the increase in H3 absorption. The corresponding data for the decrease in ND1 and increase in H3 are shown by the circles.

D. Type Ib diamond

In our as-irradiated synthetic type Ib diamonds the ND1 absorption was five to ten times greater than GR1 absorption. In the first stages of annealing the GR1 band tended to increase in intensity while the ND1 band decreased monotonically [Fig. 4(b)]. During the annealing the 1.945-eV band of the NV center is created, Fig. 8. There were no detectable variations in widths of the GR1, ND1, or NV lines during the anneal.

IV. VACANCY MIGRATION ENERGY IN TYPE IIa DIAMOND

The migration energy E_m of a vacancy can be measured from its rate of loss during isothermal annealing, as long as it is destroyed by migration to a trapping point. It is necessary to avoid loss of the vacancies through another species of defect migrating to it. It is possible that the fast initial decay of GR1 absorption (Fig. 2) is caused by the loss of vacancies by recombination with mobile self-interstitials. We concentrate here on the

slower decay process, which has decay times similar to those observed at the same temperatures in the type Ia diamonds.

The loss of vacancies in type IIa diamonds has been suggested to occur through the formation of vacancy pairs, in which case second-order kinetics would apply.¹ At higher temperatures, we assume that the formation of the vacancy aggregates observed in paramagnetic resonance² will take place initially through divacancy formation, again implying approximately second-order kinetics for the loss of vacancies. In contrast, trapping at dislocations is expected to proceed through first-order kinetics, given the small radiation doses and a high density of trapping points. The slow decay of the GR1 band in type IIa diamond could therefore be expected to obey either

$$dV/dt = -r_1 V \text{ or } dV/dt = -r_2 V^2, \quad (4.1)$$

for first- and second-order kinetics, respectively. If both capture processes have comparable importance we could expect

$$dV/dt = -r_1 V - r_2 V^2, \quad (4.2)$$

giving

$$\frac{1}{V} = \frac{\exp(r_1 t)}{V_0} + \frac{r_2}{r_1} [\exp(r_1 t) - 1], \quad (4.3)$$

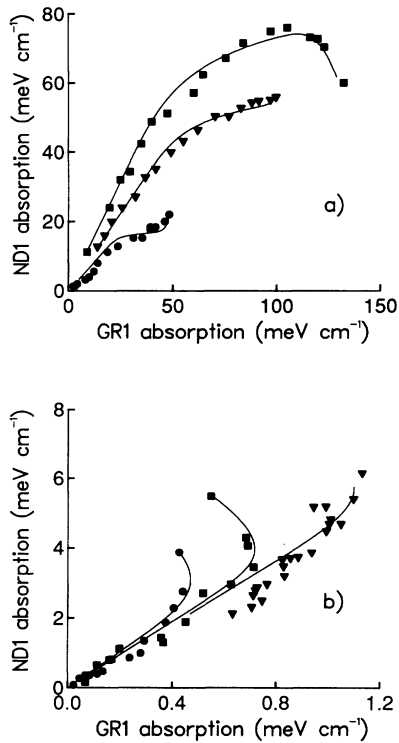


FIG. 4. Comparison in (a) three type IaA diamonds, and (b) in three type Ib diamonds, of the ND1 and GR1 absorption lines during isothermal annealing. For each sample the as-irradiated condition is shown by the point furthest from the origin, and successive annealing stages follow the curves towards the origin. The lines are calculated using the charge transfer process $V^- \rightarrow V^0 + e^-$ with V^0 being captured by the nitrogen, Eqs. (6.6a) and (6.6b) for the type Ib diamonds and Eq. (6.7) for the type IaA diamonds. In (a) two of the samples were annealed at 600°C (squares and triangles) one at 650°C (circles) and in (b) at 650°C (triangles), 750°C (squares) and 800°C (circles).

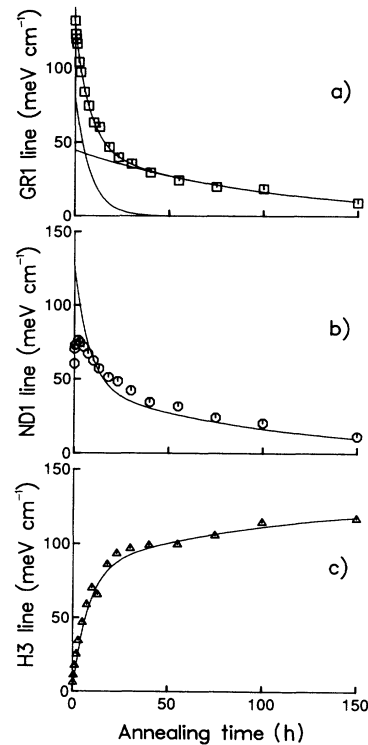


FIG. 5. Data for the isothermal annealing at 600°C of one type IaA diamond. (a) The decay of the GR1 line and (c) the growth of the H3 line are fitted using the two-exponential processes, Eqs. (5.1) and (5.2). The circles on (b) show measured data for the ND1 absorption and the line is the fit to the GR1 data from (a).

where V_0 is the initial concentration of vacancies decaying through these processes. Figure 2 shows fits to the data for first-order and second-order kinetics, and for the combined process, Eq. (4.3), which produces the best fit. However, since both first- and second-order kinetics involve the motion of V^0 , we can obtain the migration energy E_m of the vacancy from either, or from the combination, despite their different mathematical forms. Plots of $\ln r_1$ against $1/T$ for first-order kinetics, or of $\ln(r_2/A_{GR1}^0)$ against $1/T$ for second-order kinetics, yield very similar values. The values plotted in Fig. 9 are derived from fits of Eq. (4.3) and show the behavior of r_1 , for ease of comparison with the type IaA diamonds discussed next. The migration energy is determined to be

$$E_m = 2.4 \pm 0.3 \text{ meV} . \quad (4.4)$$

In these type IIa diamonds the absorption band of V^0 was observed but there was no evidence for the ND1 band of V^- , strongly suggesting that E_m is the migration energy of V^0 .

V. VACANCY MIGRATION ENERGY IN TYPE IaA DIAMOND

After irradiation, type IaA diamonds contain both V^- and V^0 centers. During annealing H3 production corre-

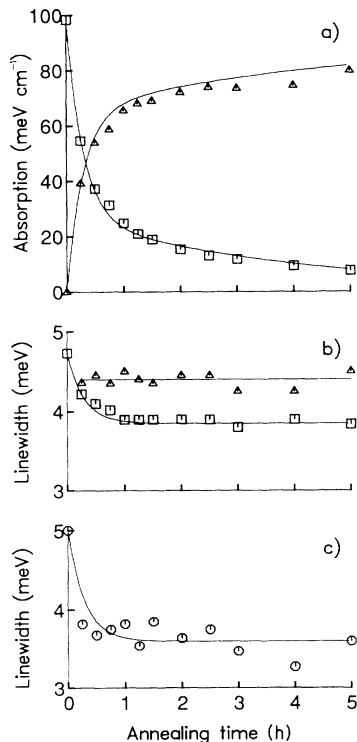


FIG. 6. (a) Destruction of GR1 (squares) and growth of H3 (triangles) in a type IaA diamond during isothermal annealing at 700°C. The lines are calculated using Eqs. (5.1) and (5.2). The full widths at half height of GR1 [squares on plot (b)], H3 [triangles on plot (b)], and ND1 [circles on plot (c)] are shown for the same diamond as used for (a). The curved lines on (b) and (c) are calculated using Eq. (7.1).

lates with loss of GR1, but not of ND1 [Fig. 3(b)]. Consequently, we will initially concentrate on the GR1 band of V^0 .

Compared to type IIa diamond, type Ia diamond has two simplifications. First, we know that at least some of the vacancies migrate to the nitrogen impurity, and secondly we can identify the end products of the annealing by the H3 and H4 absorptions. Although the *A* and *B* nitrogen aggregates act as trapping points for the migrating vacancies, we do not yet know that they are the only trapping points. However, from Eq. (2.2) the concentration of nitrogen is over two orders of magnitude greater than the vacancy concentration. Consequently the nitrogen aggregates alone are sufficient for us to expect the vacancies to decay with first-order kinetics if they migrate by a random walk. In fact the observed decays of the GR1 (V^0) line in all our type IaA diamonds are not given by a single exponential [Figs. 5(a) and 6(a)]. We find that the measured absorption A_{GR1} in the GR1 line can be accurately parametrized by the sum of two exponentials:

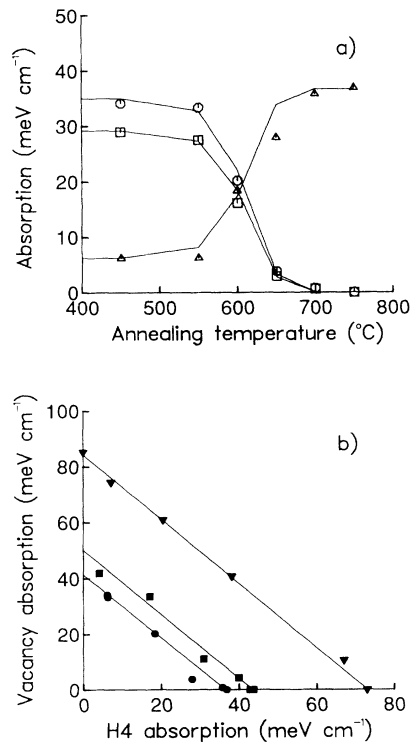


FIG. 7. (a) Data for one type IaB diamond for isochronal anneals of 1 h at each stage. The squares show the measured GR1 absorption, the triangles the measured H4 absorption, and the circles the sum ($A_{GR1} + \frac{1}{4} A_{ND1}$). The lines join points calculated at each annealing stage as described in Sec. VIII using $\tau_0 = 1.85 \times 10^{-9}$ s and a migration energy of $E = 2.2$ eV. (b) Data for three type IaB diamonds taken during isochronal annealing between 450 and 800°C with 1 h at each stage. The “vacancy absorption” is ($A_{GR1} + \frac{1}{4} A_{ND1}$) and the “H4 absorption” is the sum of the H4 absorption and a very small ($< 7\%$) contribution from H3. The straight lines have gradients corresponding to Eq. (8.1).

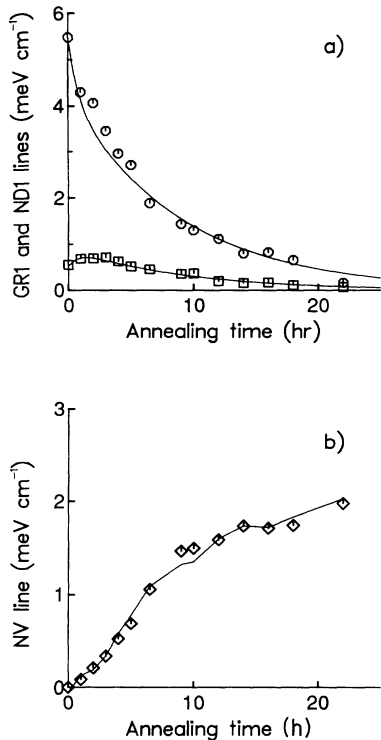


FIG. 8. Data for the isothermal annealing at 750°C of one type Ib diamond. (a) shows the absorption in the ND1 line (circles) and the GR1 line (squares). The lines are calculated using the charge transfer process $V^- \rightarrow V^0 + e^-$ with V^0 being captured by the nitrogen, Eqs. (6.6a) and (6.6b). (b) shows the measured growth of the NV absorption line (diamonds). The line joins points calculated using Eqs. (6.2), (6.3a), and (6.3b), using the data plotted in (a).

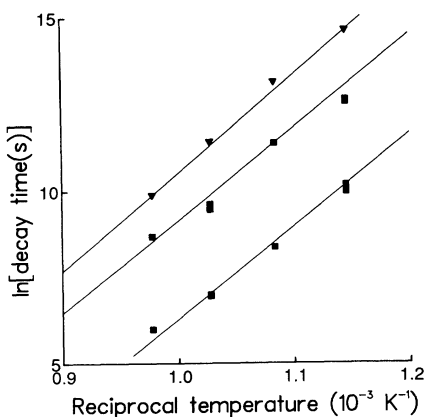


FIG. 9. Arrhenius plots of the measured exponential decay times ($1/\tau_1$) for the type IIa samples (triangles) and for the slower (τ_1) and faster (τ_2) decay times for the type IaA samples (squares). The lines are calculated for the type IIa diamonds using Eq. (5.3) with $E_m = 2.43$ eV and $\tau_0 = 2.09 \times 10^{-8}$ s. For the type IaA diamonds Eq. (5.3) has been used with the parameters of Eqs. (5.4a) and (5.4b).

$$A_{\text{GR1}} = A_{\text{GR1}}^0 \left[\left(\frac{a_1}{a_1 + a_2} \right) \exp(-t/\tau_1) + \left(\frac{a_2}{a_1 + a_2} \right) \exp(-t/\tau_2) \right], \quad (5.1)$$

where A_{GR1}^0 is the initial GR1 absorption and τ_1, τ_2 are the two exponential decay times.

The same two-speed process is seen in the growth of the 2.463 eV H3 zero-phonon line formed when the vacancies are captured by the A aggregates of nitrogen. A close fit to the absorption A_{H3} in the H3 line is obtained in all the samples without any free parameters by using the same decay times as derived from the decay of V^0 in the form

$$A_{\text{H3}} = A_{\text{H3}}^\infty \left[1 - \left(\frac{a_1}{a_1 + a_2} \right) \exp(-t/\tau_1) - \left(\frac{a_2}{a_1 + a_2} \right) \exp(-t/\tau_2) \right], \quad (5.2)$$

where A_{H3}^∞ is the strength of the H3 line after infinite annealing [Figs 5(c) and 6(a)]. The close match between the decrease in GR1 absorption and increase in H3 absorption throughout the annealing establishes that vacancies are trapped at A aggregates of nitrogen during both the fast and slow modes. Consequently both processes involve the motion of vacancies.

The fraction $a_1/(a_1 + a_2)$ of the GR1 band which is destroyed by the faster decay process varied between 0.47 and 0.8 in our seven samples. There was no correlation of $a_1/(a_1 + a_2)$ with the concentration of nitrogen in the diamonds or with the radiation dose. However, $a_1/(a_1 + a_2)$ correlated with the temperature of annealing (Fig. 10).

Figure 9 shows Arrhenius plots for the fast and slow decay times in the type IaA diamonds. In this plot we have used the measured decay times—no correction has been made for the different nitrogen concentrations in the samples, and this neglect will be partially justified in Sec. X. The straight lines through the points show that both

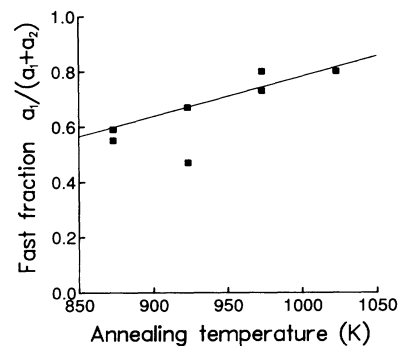


FIG. 10. Data from the isothermal annealing of seven type IaA diamonds. Squares show the fraction $a_1/(a_1 + a_2)$ of the decay of the GR1 absorption band which anneals by the faster process as a function of the annealing temperature. The outlying sample had a particularly sharp zero-phonon line.

decay rates are thermally activated in the form

$$\tau = \tau_0 \exp(E/kT), \quad (5.3)$$

and have, within experimental uncertainties, the same activation energies of

$$E_m = 2.3 \pm 0.2 \text{ eV}. \quad (5.4a)$$

The lines on Fig. 9 have been calculated with this value of E_m and with preexponential factors

$$\tau_0^f = 1.4 \times 10^{-9} \text{ s}, \quad \tau_0^s = 2.4 \times 10^{-8} \text{ s}, \quad (5.4b)$$

for the fast and slow decay processes. The uncertainty in E_m creates uncertainties in the τ_0 by a factor of 12 on either side of the quoted values.

We do not expect different charge states of a defect to have the same migration energy. Consequently, the similarities of the migration energies measured in the type IIa and IaA diamonds [Eqs. (2.3) and (5.4a)] imply that in type IaA diamonds the migration predominantly occurs through motion of V^0 centers at the temperatures used here. In the remainder of this paper we take this idea to its limit and assume that the V^- centers are static during our annealing experiments.

VI. THE ROLE OF V^-

We have suggested that V^- centers are static during the annealing, and that the loss of vacancies occurs through migration only of the neutral charge state. However, annealing does destroy the ND1 band which is characteristic of V^- [Figs. 5(b) and 8(a)]. To understand the mechanism by which V^- centers are destroyed we will make three assumptions.

- (a) All the vacancies are observed either as V^0 or as V^-
- (b) An equilibrium can be established between the two charge states
- (c) During annealing of type Ia and type Ib diamond, all the vacancies are captured at the nitrogen.

We will apply these ideas first to the type Ib diamonds, in which the negative vacancies V^- produce stronger absorption than the neutral vacancies V^0 [Fig. 8(a)]. We define f_i to relate the zero-phonon absorption A_i of the i th center with the concentration $[i]$ of that species through

$$A_i = f_i [i]. \quad (6.1)$$

Assumptions (a) and (c) then imply that the concentration of vacancies present in NV centers is equal to the changes of V^0 and V^- centers during the annealing, or, in terms of the absorption produced by these centers,

$$\frac{A_{\text{NV}}}{f_{\text{NV}}} = \frac{A_{\text{GR1}}^0 - A_{\text{GR1}}}{f_{\text{GR1}}} + \frac{A_{\text{ND1}}^0 - A_{\text{ND1}}}{f_{\text{ND1}}}. \quad (6.2)$$

We have measured A_{NV} , A_{GR1} , and A_{ND1} during the annealing of three type Ib diamonds. A least-squares fit of Eq. (6.2) to the data yields

$$f_{\text{ND1}}/f_{\text{GR1}} = 4.0 \pm 0.2, \quad (6.3a)$$

$$f_{\text{NV}}/f_{\text{GR1}} = 1.15 \pm 0.01. \quad (6.3b)$$

With these parameters Eq. (6.2) accurately reproduces the growth of A_{NV} in terms of A_{GR1} and A_{ND1} measured at each stage of the annealing [Fig. 8(b)].

The same ideas can be applied to the growth of the H3 absorption A_{H3} in type IaA diamond. A_{H3} is given by the sum of the changes in the GR1 and ND1 lines from the start of the anneal:

$$A_{\text{H3}} = f_{\text{H3}} \left[\frac{A_{\text{GR1}}^0 - A_{\text{GR1}}}{f_{\text{GR1}}} + \frac{A_{\text{ND1}}^0 - A_{\text{ND1}}}{f_{\text{ND1}}} \right]. \quad (6.4)$$

$$f_{\text{H3}}/f_{\text{GR1}} = 0.82 \pm 0.03. \quad (6.5)$$

So far in this section we have seen that the production of NV or H3 centers can be consistently accounted for in terms of the loss of V^0 and V^- centers. However, the annealing proceeds through the migration of V^0 , not of V^- . To destroy a V^- center first requires charge conversion from V^- to a mobile V^0 center. In our type Ib diamonds the ND1 and GR1 absorptions became proportional to each other at long anneal times, as shown by the data points near the origin on Fig. 4(b). This proportionality suggests that an equilibrium is eventually established between the two charge states. The movement towards equilibrium is driven by

$$\frac{d[V^-]}{dt} = \frac{-[V^-]/r + [V^0]}{\tau_{\text{con}}}, \quad (6.6a)$$

where τ_{con} is the characteristic time of the charge conversion process and r determines the final equilibrium ratio of $A_{\text{ND1}}/A_{\text{GR1}}$. The capture of the vacancies only occurs through motion of V^0 , with a characteristic time τ_{ann} :

$$\frac{d[V^0]}{dt} = -\frac{[V^0]}{\tau_{\text{ann}}} - \frac{d[V^-]}{dt}, \quad (6.6b)$$

where the last term allows for the charge conversion between V^0 and V^- . The lines through the experimental points on Figs. 4(b) and 8(a) have been calculated using Eqs. (6.6a) and (6.6b) with $f_{\text{ND1}}/f_{\text{GR1}} = 4$. For the temperatures of interest here $\tau_{\text{con}} \leq \tau_{\text{ann}}$. Consequently the loss of the vacancies is rate limited by their migration energy rather than by the charge conversion time.

In type IaA diamond the ND1 and GR1 lines also come into equilibrium after sufficient annealing, the equilibrium ratio increasing as the radiation damage initially present increases [Fig. 4(a)]. We saw in Sec. V that some V^0 centers are captured by the nitrogen with a shorter characteristic time than other V^0 centers. By the time the V^- and V^0 centers have come into their final equilibrium ratio, the more rapidly annealing V^0 centers have been destroyed, Fig. 5. Evidently it is possible for equilibrium to be achieved amongst the slowly decaying vacancies. The data can be fitted by modifying Eqs. (6.6a) and (6.6b) so that the V^- centers come into charge equilibrium with the slowly decaying component V_s^0 of V^0 and the fast and slow components of V^0 are captured by the nitrogen with characteristic times τ_{ann}^f and τ_{ann}^s :

$$\begin{aligned} \frac{d[V^-]}{dt} &= \frac{-[V^-]/r + [V_s^0]}{\tau_{\text{con}}}, \\ \frac{d[V^0]}{dt} &= -\frac{[V_s^0]}{\tau_{\text{ann}}^s} - \frac{[V_f^0]}{\tau_{\text{ann}}^f} - \frac{d[V^-]}{dt}. \end{aligned} \quad (6.7)$$

Again the fits [Fig. 4(a)] require $f_{\text{ND1}}/f_{\text{GR1}} = 4$.

Examination of the data for types IaA and Ib diamond shows that they cannot be fitted if only a one-way conversion of $V^- \rightarrow V^0$ is used; the charge transfer between V^0 and V^- must be reversible. Also, in the type Ia diamonds an accurate fit is obtained only if the V^- centers come into equilibrium with the slowly decaying component of V^0 , not with all the surviving V^0 centers. It is the existence of the two-stage annealing and the equilibrium only with the slow decaying component which results in the possibility of S-shaped curves on Fig. 4(a).

We now see why the growth of H3 in type IaA diamond may be calculated from the loss of GR1 absorption without allowance for the ND1 band, Eq. (5.2) and Fig. 3(b). After irradiation the ND1 absorption is typically ~ 0.4 of the GR1 absorption, corresponding to an order of magnitude fewer V^- centers than V^0 , Eqs. (6.1) and (6.3a). The behavior of this small concentration of V^- centers is almost irrelevant to the total behavior of all the vacancies.

VII. LOCATION OF THE VACANCIES IN TYPE IaA DIAMOND

In Sec. V we showed that the decay of the GR1 band in type IaA diamond can be described very simply using the sum of a faster decay and a slower decay. We will continue to use this description, even though the use of two (and only two) decay processes is probably a gross oversimplification.

If each vacancy had two independent methods of decay, the decay would be given by a single exponential in time with a characteristic time τ given by a sum of the reciprocals of the individual decay times in the form $1/\tau = 1/\tau_1 + 1/\tau_2$. A sum of two exponential curves could occur if each vacancy decays either by the faster process or by slower process. Since the growth of the H3 (N-V-N) centers is also given by the sum of two saturating exponentials [Figs. 5(c) and 6(a)], both the faster and the slower processes involve the motion of vacancies to the nitrogen.

Further insight into the two annealing rates observed in type IaA diamonds comes from the variation of the full widths at half height of the GR1 and ND1 lines during the anneal. In all cases the lines sharpen during the faster anneal process. Figure 6(b) shows linewidth data for a sample whose GR1 and H3 absorptions are shown in Fig. 6(a). The GR1 width $\Gamma(t)$ at anneal time t can be adequately described with no adjustable parameters using the faster decay time τ_1 obtained from Eq. (5.1) in the form

$$\Gamma(t) = \Gamma_{\infty} - (\Gamma_0 - \Gamma_{\infty})[1 - \exp(-t/\tau_1)], \quad (7.1)$$

where Γ_0 and Γ_{∞} are the widths observed at the start and near the end of annealing. The ND1 linewidth obeys a

similar dependence [Fig. 6(c)]. In contrast, Fig. 6(b) shows that the H3 linewidth is essentially constant during the anneal—in some samples the H3 width decreases very slightly during the annealing, in others it increases a little during the first stages of annealing. However, the changes in width of the H3 line are always small compared to those of the GR1 and ND1 lines. (Note that we cannot obtain the width of the H3 line immediately after irradiation, since it is only created after some annealing.) The “3H” transition on Fig. 1(a) is not the H3 transition—3H occurs at a distinctly different center, and is destroyed rapidly on annealing.

The widths of zero-phonon lines are caused predominantly by the range of perturbations, particularly by strain perturbations, of the optical centers in their different local environments in the samples.⁴⁸ The experimental data show that some vacancies are more highly strained than others, and that the highly strained centers are amongst those trapped faster at the nitrogen impurity. Nitrogen is known to be a major source of strain in type Ia diamonds,¹⁵ and its effect on the H3 linewidth is known.⁴⁹ It is possible that the additional GR1 and ND1 linewidths at the start of the anneal are caused by the faster-annealing V^0 centers being in regions of particularly high nitrogen content. This possibility may be excluded since H3 centers formed in regions of high nitrogen would give zero-phonon lines which would be broad at the start of the anneal and would progressively sharpen as V^0 centers were formed randomly in the crystal; this variation in width is not observed [Fig. 6(b)]. A more likely explanation of the linewidth behavior is that some V^0 centers are created close to a nitrogen aggregate. In a quasirandom motion they would be more likely to be captured first, sharpening the GR1 and ND1 zero-phonon lines at rates characterized by the fast decay time.

We can estimate the fraction of the vacancies in the more highly strained environments by using a simple model. We assume that a fraction f of all the vacancies is created near the nitrogen, and for simplicity we assume that these vacancies are equally perturbed. Both the GR1 and ND1 transitions involve degenerate electronic states which are split by the symmetry-lowering components of the perturbation. Consequently their zero-phonon lines are discretely perturbed through energies $\pm\Delta E$ from the ideal zero-phonon energy. In addition the background strain in the diamonds is assumed to produce the linewidths Γ_{∞} observed towards the end of the anneals. The observed line at the start of annealing is therefore assumed to consist of a central component plus two outer components displaced by $\pm\Delta E$ and each containing $f/2$ of the total absorption; we will use Lorentzian line shapes of widths Γ_{∞} for the three peaks. As a specific example we apply this model to the ND1 data of Fig. 6(c). The background linewidth of $\Gamma_{\infty} = 3.6$ meV is increased to 5.6 meV by the discretely perturbed V^- centers. These widths do not uniquely define both f and ΔE . However, they do define a lower limit to f , $f \geq 0.4$ corresponding to $\Delta E \leq 2.4$ meV.

The value of ΔE can be used to estimate the proximity of these highly perturbed V^- centers to the nitrogen. The ND1 zero-phonon line is known to be perturbed par-

ticularly by shear stress,¹² a shear strain e_{xy} producing perturbations of $\Delta h\nu = Cc_{44}e_{xy}$, where C has been measured to be 3.9 meV/GPa, and the elastic constant $c_{44} = 578$ GPa.⁵⁰ The strain produced by a nitrogen aggregate can be estimated by using elastic continuum theory and regarding the aggregate as a point defect. The shear strain at a distance r from the nitrogen is then $e_{xy} = -3xyA/r^5$ where the size mismatch of the nitrogen in the diamond crystal is given by A . A is related to the lattice expansion $\Delta V/V$ produced by a concentration ρ of aggregates by $\Delta V/V = 12\pi A\rho(1-p)/(1+p)$ where $p = 0.2$ is an estimated Poisson's ratio.⁵¹ The use of a spherical point defect to represent the nitrogen aggregate is necessary because we only know the isotropic expansion of the lattice and have no information about the axial perturbations produced by the nitrogen. Combining the known lattice expansion,¹⁵ with the most recent nitrogen calibration data,¹⁶ $A = 1.1 \times 10^{-31}$ m³. Using this theory we calculate that to generate the extra width of ~ 2.4 meV in the ND1 line requires the ND1 center to be about 0.7 nm from the nitrogen, i.e., at only four or five times the C-C bond length of 0.154 nm.

This estimate suggests that about $\geq 40\%$ of the vacancies are found, after the radiation damage, only a few atomic spacings from the nitrogen. The precise values cannot be trusted, but they suggest considerable localization of vacancies near the nitrogen. For comparison, with the concentrations of A aggregates used here (typically 2.5×10^{19} cm⁻³), the total volume within a distance 0.7 nm of a nitrogen aggregate is $\sim 3\%$ of the whole volume of the crystal. Apparently, vacancies are preferentially created near to the nitrogen. To test this deduction we have irradiated a type IaA diamond containing 1.8×10^{20} cm⁻³ nitrogen and a type IIa diamond, carefully using the same irradiation conditions and doses [Figs. 1(a) and 1(b)]. Using Eq. (6.3a) to convert the measured ND1 absorption into equivalent GR1 absorption, the ratio of the vacancy production in the type Ia and IIa diamonds was

$$[V_{\text{Ia}}]/[V_{\text{IIa}}] = 1.6 \pm 0.1. \quad (7.2)$$

This observed enhanced production in type Ia diamond would result in a fraction $(1.6 - 1)/1.6 = 0.38$ of the vacancies being strongly perturbed, very close to the lower limit of our simple estimate ($f \geq 0.4$).

VIII. ISOCHRONAL ANNEALING OF TYPE IaB DIAMOND

As a check on the analysis of the isothermal annealing in type IaA and type Ib diamond we will apply the same ideas to the isochronal annealing data of type IaB diamonds in which H4 centers are created when the vacancies are trapped at the B aggregates of nitrogen. The assumptions at the start of Sec. VI imply that as long as the concentration of nitrogen is high enough that the B aggregates are the dominant trap for the vacancies, the loss of V^0 and V^- centers should correlate linearly with the growth of H4 centers. From Eq. (6.3a), the concentration of V^0 and V^- is proportional to the $A_{\text{GR1}} + \frac{1}{4}A_{\text{ND1}}$, and as shown in Fig. 7(b) this quantity decreases linearly with

the growth of the H4 absorption for each of the three samples. The gradients are equal and give

$$f_{\text{H4}}/f_{\text{GR1}} = 0.87 \pm 0.01, \quad (8.1)$$

close to the value in Eq. (6.4) for the similar H3 center.

To fit the isochronal annealing data of the type IaB diamonds with a minimum number of adjustable parameters, we assume that at each temperature the vacancies anneal with a characteristic time τ which is thermally activated: $\tau = \tau_0 \exp(E/kT)$. Figure 7(a) shows that close fits to the isochronal data can be made, treating τ_0 and E as adjustable parameters. A least-squares fit to the data for the loss of GR1 and ND1 absorption in the three samples yields

$$E = 2.2 \pm 0.2 \text{ eV} \quad (8.2)$$

in close agreement with the values of Eqs. (4.4) and (5.4a) derived from the isothermal data.

Finally we see in Fig. 7 that the growth of the H4 absorption may be represented without further adjustable parameters by analogy with Eq. (6.4):

$$A_{\text{H4}} = A_{\text{H4}}^0 + f_{\text{H4}} \left[\frac{A_{\text{GR1}}^0 - A_{\text{GR1}}}{f_{\text{GR1}}} + \frac{A_{\text{ND1}}^0 - A_{\text{ND1}}}{f_{\text{ND1}}} \right], \quad (8.3)$$

where A_{H4}^0 allows for any absorption in the H4 line which is present in the type IaB samples before irradiation, and $f_{\text{H4}}/f_{\text{GR1}}$ is known from Eq. (8.1). The equation accurately describes the growth of the H4 band (Fig. 7).

IX. DETAILED BALANCE

In Secs. VI and VIII, two of the assumptions used to relate the growth of H3, H4, and NV with the loss of vacancies were that all the vacancies are present either as V^0 or as V^- , and they are all eventually trapped at the nitrogen and at no other traps. These same assumptions allow us to link the strengths of the vacancy-related absorption bands to the radiative lifetimes of the transitions using detailed balance which gives

$$\int_{\text{band}} dE \mu(E) = \frac{\pi^2 c^2 \hbar^3}{9} \left[\frac{n^2 + 2}{n} \right]^2 \frac{g_e}{g_g} \frac{1}{\tau_r E^2} [C], \quad (9.1)$$

where $\int_{\text{band}} dE \mu(E)$ is the total absorption in a vibronic band, τ_r is the radiative lifetime and E is the mean energy of the luminescence transition, g_e and g_g are the degeneracies of the excited and ground states of the transition, $[C]$ is the concentration of the optical center, and n is the refractive index at the optical center. For convenience, all quantities are expressed in S.I. units. Equation (9.1) contains known physical constants (the Planck constant and the speed of light) but n is difficult to define. We argue that all the vacancy centers discussed here may be regarded either as simply vacancies or as vacancies perturbed by neighboring nitrogen atoms,⁵² so that n is similar for each center. In our experiments we have measured the absorption A_i in each zero-phonon line, which

is a fraction z_i of the total absorption in each band. Values of z_i , g_e , g_g , and τ_r for each band are listed in Table I.

First we rationalize the data for the production of H3 and H4 centers. By combining Eqs. (6.5) and (8.1) for the annealing of types IaA and IaB diamond, we see that the ratio of the zero-phonon absorptions produced by one H3 center and one H4 center is

$$f_{H3}/f_{H4} = 0.95 \pm 0.05. \quad (9.2)$$

From Eq. (9.1) and Table I, the ratio is expected to be

$$\left(\frac{f_{H3}}{f_{H4}} \right) = \left(\frac{g_e^{H3}}{g_g^{H3}} \frac{z_{H3}}{\tau_{H3} E_{H3}^2} \right) / \left(\frac{g_e^{H4}}{g_g^{H4}} \frac{z_{H4}}{\tau_{H4} E_{H4}^2} \right) = 0.84 \pm 0.9, \quad (9.3)$$

in agreement with Eq. (9.2) within the uncertainties. Similarly, Eqs. (6.3b) and (6.5) show that one H3 center produces 0.71 ± 0.03 times the zero-phonon absorption of one NV center. From Eq. (9.1) and Table I we would expect 1.0 ± 0.07 . These figures do not agree within the experimental errors, and possibly demonstrate the limitations of these simple detailed balance arguments. It is known that when Eq. (9.1) is applied to optical centers in silicon, the group-IV semiconductor next to diamond, its uncertainty is up to a factor of 2.⁵³ Within these limits, the similarity of the measured and predicted ratios from independent data using both synthetic diamonds and natural diamonds with very different geological histories suggests that the underlying assumptions are valid—that essentially all the vacancies in these diamonds are either V^0 or V^- , and that during migration virtually all are trapped at nitrogen.

Similar arguments allow us to estimate the true radiative decay time τ_{GR1} of the GR1 luminescence band. τ_{GR1} is not known, only the measured decay time (~ 2.5 ns as $T \rightarrow 0$ K) which is affected by strong nonradiative processes.⁹ Equation (6.5) gives the measured ratio A_{H3}/A_{GR1} of absorption in the H3 and GR1 lines for the same concentrations of N-V-N and V^0 centers. Using Eq. (9.1), it can be rewritten as

$$\left(\frac{f_{H3}}{f_{GR1}} \right) = \left(\frac{g_e^{H3}}{g_g^{H3}} \frac{z_{H3}}{\tau_{H3} E_{H3}^2} \right) / \left(\frac{g_e^{GR1}}{g_g^{GR1}} \frac{z_{GR1}}{\tau_{GR1} E_{GR1}^2} \right) = 0.82. \quad (9.4)$$

Evaluating Eq. (9.4) for τ_{GR1} gives

$$\tau_{GR1} \sim 42 \text{ ns}. \quad (9.5a)$$

Similarly, combining Eq. (6.3b) and the parallel of Eq. (9.4) for the conversion of V^0 to an NV center gives

$$\tau_{GR1} \sim 28 \text{ ns}. \quad (9.5b)$$

The radiative decay time of the GR1 band in the absence of competing nonradiative channels is therefore expected to be $\sim 35 \pm 7$ ns, of a similar magnitude to values typical for diamond (Table I).

Direct application of Eq. (9.1) to the GR1 center, and using $n = 2.44$ as for perfect diamond and $\tau_{GR1} = 35$ ns, we obtain $f_{GR1} = 2 \times 10^{-15}$ meV cm². In the type IIa diamond used for Fig. 1(a) the GR1 absorption was $A_{GR1} = 45$ meV cm⁻¹ after a dose of 3×10^{17} cm⁻³ 2 MeV electrons cm⁻², implying a vacancy production rate of 0.075 cm⁻¹. From Eq. (2.2) the measured compensation rate of boron acceptors in *p*-type diamond during 2-MeV irradiation is 4 times larger, but may be caused by both vacancy and self-interstitial effects; however, the evidence is that Eq. (9.1) underestimates the concentration of the centers by about at least a factor of 2.

X. DISCUSSION

The migration energy of V^0 has been measured to be $E_m = 2.3 \pm 0.3$ eV [Eqs. (4.4), (5.4a), and (8.2)]. In unpublished work,⁵⁴ Palmer annealed one type IIa diamond at successively higher temperatures of 500, 600, and 700 °C and derived two activation energies for the destruction of the V^0 centers, 1.62 and 2.35 eV. The latter value is very close to our value of E_m , and the former may be associated with the fast destruction of some V^0 centers during the first stages of annealing. Bernholc *et al.*⁵⁵ have calculated the difference in energy between having a carbon atom at the saddle point between two vacant sites and the T_d

TABLE I. Relevant properties of the vacancy centers.

Name	Energy (eV)	Center	z_i^a	g_g^b	g_e^b	τ_r^c (ns)	References
GR1	1.673	V^0	0.042	2	3	2.55 ± 0.1	3,4,9
ND1	3.150	V^-	0.041	1	3	n/a^d	3,12
NV	1.945	N-V	0.024	1	2	130 ± 0.5	3,22,35
H3	2.463	N-V-N	0.05	1	1	16.7 ± 0.5	3,40,42
H4	2.498	$V+B^e$	0.05	1	1	19.1 ± 1.0	3,41,43

^a z_i is the fraction, at low temperature, of the measured absorption in each vibronic band which lies in the zero-phonon line.

^b g_g and g_e are the orbital degeneracies of the ground and excited states of the optical transition.

^c τ_r is the radiative decay time as measured at low temperature; for the GR1 band τ_r is reduced from its true value by nonradiative decay channels.

^dNo luminescence has been detected from the 3.150 eV transition.

^e*B* indicates the *B* nitrogen aggregate.

vacancy, obtaining 1.9 eV with an estimated uncertainty of 0.1 eV. To convert this value into the migration energy requires the addition of the Jahn-Teller stabilization energy in the ground state of V^0 , which from the vibronic band shapes is about 0.2 eV.⁵⁶ Their value is then $E_m = 2.1 \pm 0.1$ eV, in close agreement with our experimental value.

In Sec. VII we showed that vacancy production by 2-MeV electrons is about 40% larger in type Ia diamond than in type IIa diamond, and that the extra vacancies are in highly perturbed environments within a few atomic radii of the nitrogen aggregates. We concluded that preferential creation of vacancies occurs in a small volume near the A nitrogen aggregates. The preferential creation is presumably not a consequence of lattice distortions near the nitrogen since the migration energy for these localized vacancies is indistinguishable from that of the randomly created vacancies, suggesting that there is no weakening of the lattice near the nitrogen. One possibility is as follows. During electron irradiation many of the self-interstitials undergo rapid correlated recombination with their vacancies, so that only a fraction of the atomic displacements survive to be observed in the optical measurements. The nitrogen may reduce the correlated recombination, so enhancing the rate of production of observable damage. For example, the nitrogen could capture the self-interstitial, but then we would not expect to get a standard H3 center when the vacancy was captured at the same (nearby) nitrogen aggregate. Alternatively, the nitrogen could modify the electrical charges on the vacancy and self-interstitial increasing the probability of their separating. Further work is required to understand the magnitude of the correlated recombination, for example, by measuring the production of damage in pure diamond as a function of temperature, for which existing data are sparse.^{45,46}

Although $\sim 40\%$ of the vacancies are created in the vicinity of the A nitrogen aggregates, between 55% and 80% anneal by the faster process, the percentage increasing with the annealing temperature (Fig. 10). We suggest that a substantial fraction of the vacancies, including those preferentially created near the A aggregates, are captured relatively rapidly by neighboring nitrogen. For this reason it was appropriate to plot on Fig. 9 the *measured decay time* rather than the measured decay time multiplied by the concentration of the nitrogen, at least for the faster annealing component. The fact that the fraction of vacancies annealing faster increases with the annealing temperature suggests that the energy of the vacancy in its T_d site increases as it moves towards the nitrogen—the vacancy moves “uphill” to the nitrogen. The energy gradient must be small enough not to affect the measured migration energy of the vacancy [Eqs. (4.4) and (5.4a)]. It is possible that this energy gradient is the cause of the unexpectedly large value of the faster anneal time τ_0^f of Eq (5.4b). Assuming a typical vibration frequency for vacancies in diamond of 10^{13} Hz (40 meV), $\tau_0^f = 1.4 \times 10^{-9}$ s corresponds to 1.4×10^4 jumps, for vacancies which are created within a few atomic sites of the nitrogen trapping points. The kinetics require further detailed modeling.

When the vacancy is captured by the N-N nitrogen aggregate in type Ia diamond, giving N-N- V , it must convert to the N- V -N structure of the H3 center—some restructuring is necessary since the observed point group of H3, C_{2v} , is not a subgroup of the D_{3d} symmetry of the A aggregate.^{25,40} If the conversion requires a formation barrier of energy E_f to be overcome, the mean time for the final conversion is expected to be $\tau_f = \tau_{f0} \exp(E_f/kT)$. Since the conversion involves one atomic jump, we expect the characteristic time τ_{f0} to be of the order of the time period of an atomic vibration, which we assume is $\sim 10^{-13}$ s as is typical for vacancy complexes in diamond. We can therefore model the production of H3 centers by the differential equations

$$d[\text{N-N-}V]/dt = [V]/\tau_m - [\text{N-N-}V]/\tau_f,$$

$$d[\text{N-}V\text{-N}]/dt = [\text{N-N-}V]/\tau_f,$$

where τ_m is the characteristic capture time of vacancies at the A aggregate. These equations yield

$$[\text{N-}V\text{-N}] = [V]_0 \frac{\tau_m(1 - e^{-t/\tau_m}) - \tau_f(1 - e^{-t/\tau_f})}{(\tau_m - \tau_f)}, \quad (10.1)$$

where $[V]_0$ is the initial concentration of vacancies. With finite τ_f there is a slower initial growth of N- V -N centers than loss of vacancies as the vacancies are bottlenecked in the N-N- V configuration. We do not observe this slow initial rise in H3 absorption, but our data only allow us to deduce that $E_f < 2.8$ eV, and it is even possible that the final conversion is exothermic.

We have shown in Sec. VI that the annealing of V^- proceeds by conversion first to V^0 . Charge transfer processes are inevitably specimen dependent since the electron liberated in the ionization $V^- \rightarrow V^0 + e^-$ must be trapped elsewhere. We have no knowledge of the nature of these traps. In type IaA diamonds the charge transfer processes become more apparent with increasing radiation dose [Fig. 4(a)], possibly through the creation of different electron traps (e.g., interstitial clusters) with increasing dose. We have noted that in type IaA diamonds the V^0 and V^- centers come into charge equilibrium for those vacancies which are captured relatively slowly at the nitrogen. Qualitatively it appears that vacancies created relatively close to the nitrogen aggregates have their charge states pinned by the nitrogen, but our data are too sparse to make this statement quantitative. However, the charge transfer process has allowed us to determine the relative absorption in the GR1 and ND1 bands per vacancy, $f_{\text{ND1}}/f_{\text{GR1}} = 4.0 \pm 0.2$ and that value agrees with the value we have derived from the conversion of V^0 and V^- to NV and H3 centers. A similar value can be deduced from published data of Dyer and du Preez.¹⁴ They studied the interconversion of GR1 and ND1 bands by heat treatments and photochromic effects, using very low resolution measurements. They quoted values for the total absorption in the vibronic bands, after subtracting underlying absorption, which convert into our nomenclature in the range $f_{\text{ND1}}/f_{\text{GR1}} = 5.5 - 10$. It would be useful to repeat the Dyer and du Preez experiments using

modern equipment.

Finally we note that throughout this paper it has been possible to ignore the interstitials, except possibly for the rapid initial decay of V^0 centers in type IIa diamonds. It has long been known that irradiating type Ia diamond with γ rays creates highly perturbed V^0 centers and, consequently, broad GR1 bands.¹ Annealing these diamonds can result in a loss of 75% of the V^0 centers with no creation of H3 centers, consistent with the suggestion that vacancy-interstitial recombination is occurring in this initial annealing phase.¹ We have shown that in type I diamonds irradiated at room temperature with 2-MeV electrons there is no evidence for vacancy-interstitial recombination—the loss of vacancy centers correlates with the creation of H3, H4, or NV centers. Consequently we have established one simplification in radiation damage studies of type I diamond, that the reaction paths of self-interstitials and vacancies do not interfere with each other.

XI. SUMMARY

In a pure crystal we expect the vacancies to be found in one charge state. In the relatively pure type IIa diamond V^0 is observed, but not V^- . The migration energy of the vacancy measured in type IIa has therefore been assigned to the value for V^0 . In type IaA diamond, containing pairs of substitutional nitrogen atoms, we have measured the same vacancy migration energy, implying that V^0 is the mobile species even though, for reasons which we do not understand, both V^0 and V^- exist in these diamonds. In nitrogen-containing diamonds our annealing data are consistent with a charge transfer occurring, possibly during the heat treatments, between V^0 and V^- . The static V^- is destroyed on annealing by first converting to the mobile V^0 . From the reversible charge transfers we have derived a value for the relative absorption per vacancy in the two bands. The value agrees with an independent assessment obtained by comparing the destruction of V^0 and V^- with the production of H3 (or NV) centers in type Ia (or Ib) diamond. We have shown that irradiating type Ia diamond with 2-MeV electrons creates about 10 times more V^0 centers than V^- centers. The lack of reported positron annihilation at V^- in irradiated type Ia diamond is consistent with this result.⁴⁴ The self-consistent picture emerging here suggests that the underlying assumptions are valid—that effectively all the vacancies in types Ia and Ib diamond are present either in their neutral or singly negative charge states, and that during annealing the vast majority of the vacancies are trapped at the nitrogen impurity. The same assumptions

have been used to determine a value for the true radiative lifetime τ_{GR1} (in the absence of the nonradiative channels) of the GR1 band and have given two independent, and closely agreeing, values of τ_{GR1} . It appears that, as far as vacancy migration is concerned, type IaA diamonds which contain mainly A nitrogen aggregates and type Ib diamonds can be regarded as high-quality diamond crystals with one dominant impurity, nitrogen, and no other significant crystal flaws.

In type Ia diamonds there is an increase in vacancy production by $\sim 40\%$ over type IIa diamond as a result of some of the vacancies being created close to (within a few lattice spacings of) the nitrogen impurity. The localized vacancies are rapidly destroyed on annealing by a relatively fast capture at the nitrogen. With increasing temperature of anneal the fraction of the vacancies undergoing this fast anneal increases, suggesting that, in addition to the localized vacancies some of the other vacancies can also move rapidly to the nitrogen. Possibly the vacancy energy increases slightly towards the nitrogen, so that there is a short-range repulsion of the vacancies from the nitrogen. However, we have no evidence of an energy barrier hindering the final formation of the H3 centers.

This work has demonstrated that radiation effects in diamond, which were first systematically studied over thirty years ago, are still not fully understood. For example, we need to determine why there is a greater creation of vacancies near the nitrogen in the common type IaA diamonds, and why there is a fixed ratio of the concentrations of V^0 and V^- in these diamonds. We have shown that it is possible, in types Ia, Ib, and IIa diamonds, to consider all the vacancies as being in either the neutral or negative charge state. The dynamics of the reversible charge transfers between V^0 and V^- require further investigation, to locate the ground states of the centers relative to the electronic band states of the host lattice. This leaves the positive charge state of the vacancy as an essentially unexplored center; since natural *p*-type semiconducting natural diamond usually has low levels of acceptors (10^{17} cm^{-3}), V^+ may be more readily studied by irradiation of heavily doped *p*-type synthetic diamond.

ACKNOWLEDGMENTS

We thank G. S. Woods and I. Kiflawi for providing some of the diamonds used in this work, and the former for measuring the nitrogen concentrations in some of the samples. Financial support was provided by the Science and Engineering Research Council and by De Beers Industrial Diamond Division.

*Present address: National Institute for Research in Inorganic materials, 1-1 Namiki, Tsukuba, Ibaraki 305, Japan.

¹C. D. Clark, R. W. Ditchburn, and H. B. Dyer, Proc. R. Soc. London Ser. A **234**, 363 (1956); **237**, 75 (1956).

²C. D. Clark, E. W. J. Mitchell, and B. J. Parsons, in *The Properties of Diamond*, edited by J. E. Field (Academic, London, 1979), pp. 23–77.

³G. Davies, Rep. Prog. Phys. **44**, 787 (1981).

⁴C. D. Clark and J. Walker, Proc. R. Soc. London Ser. A **234**, 241 (1973).

⁵A. M. Stoneham, Solid State Commun. **21**, 339 (1977).

⁶J. Walker, L. A. Vermeulen, and C. D. Clark, Proc. R. Soc. London Ser. A **341**, 253 (1974).

⁷L. A. Vermeulen, C. D. Clark, and J. Walker, in *Lattice Defects in Semiconductors, 1974*, edited by F. A. Huntley, IOP Conf. Proc. No. **23** (Institute of Physics and Physical Society, Lon-

- don, 1975), p. 294.
- ⁸C. D. Clark, P. J. Dean, and P. V. Harris, Proc. R. Soc. London Ser. A **277**, 312 (1964).
- ⁹A. T. Collins, J. Phys. C **20**, 2027 (1987); G. Davies, M. F. Thomaz, M. H. Nazaré, M. M. Martin, and D. Shaw, *ibid.* **20**, L13 (1987).
- ¹⁰J. Isoya, H. Kanda, Y. Uchida, S. C. Lawson, H. Itoh, and Y. Morita, Phys. Rev. B **45**, 1436 (1992).
- ¹¹G. Davies, Nature (London) **269**, 498 (1977).
- ¹²G. Davies and E. C. Lightowers, J. Phys. C **3**, 650 (1970).
- ¹³R. G. Farrer and L. A. Vermeulen, J. Phys. C **5**, 2762 (1972).
- ¹⁴H. B. Dyer and L. du Preez, J. Chem. Phys. **42**, 1898 (1965).
- ¹⁵W. Kaiser and W. L. Bond, Phys. Rev. **115**, 857 (1959).
- ¹⁶G. S. Woods, G. C. Purser, A. S. S. Mtinkulu, and A. T. Collins, J. Phys. Chem. Solids **51**, 1191 (1990).
- ¹⁷R. M. Chrenko, H. M. Strong, and R. E. Tuft, Philos. Mag. **23**, 213 (1971).
- ¹⁸W. V. Smith, P. P. Sorokin, I. L. Gelles, and G. J. Lasher, Phys. Rev. **115**, 1546 (1959).
- ¹⁹A. R. Lang, A. P. W. Makepeace, M. Moore, and W. Wierzchowski, in *New Diamond Science and Technology*, edited by R. Messier, J. T. Glass, J. E. Butler, and R. Roy (Materials Research Society, Pittsburgh, 1991), p. 557.
- ²⁰A. Mainwood, J. Phys. C **12**, 2543 (1979); P. R. Briddon, M. I. Heggie, and R. Jones, Mater. Sci. Forum **83–87**, 457 (1992).
- ²¹R. G. Farrer, Solid State Commun. **7**, 685 (1969).
- ²²G. Davies and M. F. Hamer Proc. R. Soc. London Ser. A **348**, 285 (1976).
- ²³W. J. P. van Enkevort and E. H. Versteegen, J. Phys. Condens. Matter **4**, 2361 (1992).
- ²⁴T. Evans and Z. Qi, Proc. R. Soc. London Ser. A **381**, 159 (1982).
- ²⁵G. Davies, J. Phys. C **9**, L537 (1976).
- ²⁶P. Denham, E. C. Lightowers, and P. J. Dean, Phys. Rev. **161**, 762 (1967).
- ²⁷A. Mainwood, F. Larkins, and A. M. Stoneham, Solid State Electron. **21**, 1431 (1979).
- ²⁸Y. M. Kim and G. D. Watkins, J. Appl. Phys. **42**, 722 (1971); Y. M. Kim, Y. H. Lee, P. Brosious, and J. W. Corbett, in *Radiation Defects and Damage in Semiconductors, 1972*, edited by J. E. Whitehouse, IOP Conf. Proc. No. 16 (Institute of Physics and Physical Society, London, 1973), p. 202.
- ²⁹I. T. Flint and J. N. Lomer, Physica **116B**, 183 (1983).
- ³⁰J. Koike, T. E. Mitchell, and P. M. Parkin, Appl. Phys. Lett. **59**, 2515 (1991); J. Koike, P. M. Parkin, and T. E. Mitchell, *ibid.*, **60**, 1450 (1992).
- ³¹A. T. Collins, G. Davies, H. Kanda, and G. S. Woods, J. Phys. C **21**, 1363 (1988).
- ³²S. C. Lawson, G. Davies, A. T. Collins, and A. Mainwood, J. Phys. Condens. Matter. **4**, 3439 (1992).
- ³³J. N. Lomer and A. M. A. Wild, Radiat. Eff. **17**, 37 (1973).
- ³⁴A. R. Lang, in *the Properties of Diamond*, edited by J. E. Field (Academic, London, 1979), pp. 425–469.
- ³⁵A. T. Collins, M. F. Thomaz, and M. I. B. Jorge, J. Phys. C **16**, 2177 (1983).
- ³⁶D. A. Redman, S. Brown, R. H. Sands, and S. C. Rand, Phys. Rev. Lett. **67**, 3420 (1991).
- ³⁷J. H. N. Loubser and J. A. van Wyk, in *Diamond Research 1977*, edited by P. Daniel (De Beers Industrial Diamond Division, Ascot, 1977), pp. 11–14.
- ³⁸G. Davies, J. Phys. C **5**, 2534 (1972); C. D. Clark and S. T. Davey, *ibid.* **17**, L399 (1984).
- ³⁹A. T. Collins, in *Defects and Radiation Effects in Semiconductors, 1978*, edited by J. H. Albany, IOP Conf. Proc. No. 46 (Institute of Physics and Physical Society, London, 1979), p. 327.
- ⁴⁰G. Davies, M. H. Nazaré, and M. F. Hamer, Proc. R. Soc. London Ser. A **351**, 245 (1976).
- ⁴¹E. S. de Sa and G. Davies, Proc. R. Soc. London Ser. A **357**, 231 (1977).
- ⁴²M. D. Crossfield, G. Davies, A. T. Collins, and E. C. Lightowers, J. Phys. C **7**, 1909 (1974).
- ⁴³A. T. Collins, M. F. Thomaz, and M. I. B. Jorge, J. Phys. C **16**, 5417 (1983).
- ⁴⁴S. Dannefaer and D. Kerr, Diamond Related Mater. **1**, 407 (1992).
- ⁴⁵A. T. Collins, in *Radiation Effects in Semiconductors, 1976*, edited by N. B. Urli and J. W. Corbett, IOP Conf. Proc. No. 31 (Institute of Physics and Physical Society, London, 1977), p. 346.
- ⁴⁶E. A. Burgemeister, C. A. J. Ammerlaan, and G. Davies, J. Phys. C **13**, L691 (1980).
- ⁴⁷G. Davies, Proc. R. Soc. London Ser. A **336**, 507 (1974).
- ⁴⁸A. M. Stoneham, Rev. Mod. Phys. **41**, 82 (1969).
- ⁴⁹G. Davies, J. Phys. C **3**, 2474 (1970).
- ⁵⁰H. J. McSkimmin and P. Andreatch, J. Appl. Phys. **43**, 2944 (1972).
- ⁵¹J. D. Eshelby, *Solid State Physics: Advances in Research and Applications*, edited by F. Seitz and D. Turnbull (Academic, New York, 1956), Vol. 3, p. 79.
- ⁵²J. E. Lowther, J. Phys. Chem. Solids **45**, 127 (1984).
- ⁵³G. Davies, E. C. Lightowers, R. C. Newman, and A. S. Oates, Semicon. Sci. Technol. **2**, 524 (1987).
- ⁵⁴D. W. Palmer, Ph.D. thesis, University of Reading, 1961.
- ⁵⁵J. Bernholc, A. Antonelli, T. M. Del Sole, Y. Bar-Yam, and S. T. Pantelides, Phys. Rev. Lett. **61**, 2689 (1988).
- ⁵⁶G. Davies, J. Phys. C **15**, L149 (1982).